Deletion of N-myc downstream-regulated gene 2 attenuates reactive astrogliosis and inflammatory response in a mouse model of cortical stab injury

Deletion of N-myc downstream-regulated gene 2 (Ndrg2) attenuates reactive astrogliosis and inflammatory response in a mouse model of cortical stab injury

Mika Takarada-Iemata[1, 2]*, Dai Kezuka[1, 2], Toshiaki Takeichi[3], Masahito Ikawa[4], Tsuyoshi Hattori[1, 2], Yasuko Kitao[1, 2], Osamu Hori[1, 2]

[1]Department of Neuroanatomy, Kanazawa University Graduate School of Medical Sciences, Kanazawa, Ishikawa 920-8640, Japan

[2] Japan Science and Technology Agency, CREST, Kawaguchi, Saitama 332-0012, Japan

[3] Department of Legal Medicine, Kanazawa Medical University, Kahoku, Ishikawa 920-0293, Japan

[4]Research Institute for Microbial Diseases, Osaka University, Suita, Osaka 565-0871, Japan

Address correspondence and reprint requests to: Dr. Mika Takarada-Iemata
Department of Neuroanatomy, Kanazawa University Graduate School of Medical Sciences, 13-1 Takara-machi, Kanazawa, Ishikawa, 920-8640, Japan.
Tel.: 81-76-265-2162; Fax: 81-76-234-4222;
E-mail: m-tak@staff.kanazawa-u.ac.jp

Keywords: Reactive astrogliosis; Brain injury; Inflammation; Interleukin-6; Neuronal death

Running title: Ndrg2 regulates reactive astrogliosis

Abbreviations used: Ndrg2, N-myc downstream-regulated gene 2; GFAP, glial fibrillary acidic protein; IL-6, interleukin-6; STAT3, signal transducer and activator of transcription 3; NeuN, neuronal nuclei; DAPI, 6-diamidino-2-phenylindole dihydrochloride; qRT-PCR, quantitative real-time PCR; Fsk, forskolin; ssDNA, single-strand DNA

Abstract

N-myc downstream-regulated gene 2 (Ndrg2) is a differentiation- and stress-associated molecule predominantly expressed in astrocytes in the central nervous system. In this study, we examined the expression and the role of Ndrg2 after cortical stab injury. We observed that Ndrg2 expression was elevated in astrocytes surrounding the wounded area as early as day 1 after injury in wild-type mice. Deletion of Ndrg2 resulted in lower induction of reactive astroglial and microglial markers in the injured cortex. Histological analysis showed reduced levels of hypertrophic changes in astrocytes, accumulation of microglia, and neuronal death in *Ndrg2*$^{-/-}$ mice after injury. Furthermore, activation of the IL-6/STAT3 pathway, including the expression of IL-6 family cytokines and phosphorylation of STAT3, was markedly reduced in *Ndrg2*$^{-/-}$ mice after injury. In a culture system, both of *Il6* and *Gf*ap were upregulated in wild-type astrocytes treated with forskolin. Deletion of Ndrg2 attenuated induction of these genes, but did not alter proliferation or migration of astrocytes. Adenovirus-mediated re-expression of Ndrg2 rescued the reduction of IL-6 expression after forskolin stimulation. These findings suggest that Ndrg2 plays a key role in reactive astrogliosis after cortical stab injury through a mechanism involving the-positive regulation of IL-6/STAT3 signaling.

Introduction

Astrocytes, which are the most abundant cells in the central nervous system (CNS), play pivotal roles not only in the nutritional support for neurons but also in the regulation of neural activity at the tripartite synapse by modulation of extracellular transmitters and at sites of neurovascular coupling by controlling microcirculation (Araque *et al*. 1999, Iadecola and Nedergaard 2007, Schummers *et al*. 2008). In addition to these homeostatic functions in physiological conditions, astrocytes play important roles in various neuropathological conditions, including acute brain insults, such as trauma and stroke, and chronic neurodegeneration. In these conditions, astrocytes undergo hypertrophy and upregulate intermediate filament proteins such as glial fibrillary acidic protein (GFAP) and vimentin, which are referred to as reactive astrogliosis or astroglial activation. In some cases, astrocytes undergo proliferation and form a tight barrier between the injury site and the healthy areas, termed a glial scar (Sofroniew 2009). Reactive astrogliosis has both detrimental and beneficial aspects. Astrocytes are known to release inflammatory mediators and participate in innate immune reactions, and the glial scar inhibits axonal regeneration after injury (Siliver and Miller 2004, Brambilla *et al*. 2005, Widestrand *et al*. 2007). However, recent studies using mice with experimentally ablated astroglial function have demonstrated that activated astrocytes exert neuroprotection through the prevention of spread of inflammatory cells and restoration of tissue damage (Sung *et al*. 2003, Okada *et al*. 2006, Huang *et al*. 2012). Therefore, it is critical to understand the molecular mechanism underlying reactive astrogliosis in order to appropriately regulate its level and timing.

N-myc downstream-regulated gene 2 (Ndrg2) is one of the recently identified differentiation- and stress- associated genes, and a high level of Ndrg2 expression has been observed in the brain, heart, and muscle, and to a lesser extent in the liver and kidney (Qu *et al*. 2002). Ndrg2 is a cytoplasmic protein that contains several phosphorylation sites (Murray *et al*.

2004). Its structure is similar to that of the members of the alpha-beta hydrolase family, but it lacks the enzymatic sequence (Hwang *et al*. 2011); therefore, its direct function and the target proteins are still unknown. An increasing number of studies have indicated a correlation between downregulation of Ndrg2 (Lusis *et al*. 2005, Jeschke *et al*. 2012) and increased levels of proliferation (Deng *et al*. 2003, Kim *et al*. 2009b) and/or invasion (Kim *et al*. 2009a) of cancer cells. Recently, analysis using Ndrg2 gain-of-function and loss-of-function mutant mice showed that Ndrg2 regulates the vertebral specification in the differentiating somite (Zhu *et al*. 2012). In the CNS, Ndrg2 has been reported to be predominantly expressed in astrocytes (Nichols 2003, Okuda *et al*. 2008, Takeichi *et al*. 2011) and in dystrophic neurons in Alzheimer's disease (AD) (Mitchelmore *et al*. 2004). Ndrg2 has also been reported to be upregulated by adrenal steroid hormones (Boulkroun *et al*. 2002, Nichols 2003) and also in a relatively early phase after experimental ischemia (Li *et al*. 2011), while being downregulated by antidepressant and electroconvulsive treatments (Takahashi *et al*. 2005a). In our previous study, we demonstrated that Ndrg2 has an inhibitory effect on the proliferation of astrocytes in a culture system and that it is highly expressed in astrocyte-like cells in the substantia nigra of Parkinson's disease patients (Takeichi *et al*. 2011). These lines of evidence indicate that Ndrg2 expression in astrocytes could be involved in the pathogenesis of neurological disorders. In the present study, we investigated the expression of Ndrg2 and the effects of its deletion on the processes of astroglial activation, inflammatory response, and neuronal death in a cortical stab injury model.

Materials and Methods

Mice

All animal experiments were approved by the Animal Care and Use Committee of Kanazawa University (AP-122395). *Ndrg2*-deficient mice were generated through a combination of homologous recombination and Cre-mediated recombination. The targeting vector, including two loxP sites flanking exons 3 and 4 of the mouse *Ndrg2* locus and neomycin (Neo) cassette, was linearized and transfected into 129Sv/J embryonic stem cells by electroporation. Recombinant embryonic stem clones were selected with G418 antibiotic and identified by PCR analysis. Secondary confirmation was performed by Southern blotting analysis by using 2 types of [^{32}P] labeled probes for the target region of genomic DNA after digestion with *Eco*T221 (5′ probe) or *Dra*I (3′ probe). The expected sizes were 8.2 and 8.8 kb for the wild-type (WT) allele and 9.8 and 9.9 kb for the targeted allele. Two correctly targeted heterozygote embryonic stem cell clones were obtained and were microinjected into C57BL/6 blastocysts. The resulting chimeras were mated to C57BL/6 mice (Sankyo Labo Service Corporation, Tokyo, Japan) to generate F1 heterozygous offspring. Germ line transmission of *Ndrg2* mutant gene was achieved in one of those lines. *Ndrg2*$^{neo/+}$ mice were crossed with CAG-Cre transgenic mice that express Cre recombinase under a CAG promoter to generate *Ndrg2*$^{+/-}$ mice. CAG-Cre mice were kindly provided by Dr. Miyazakai (Osaka university, Osaka, Japan) (Sasaki and Miyazaki 1997). Mice were backcrossed into the C57BL/6 background for 8 generations. Genotyping was performed by PCR using tail genomic DNA. Primer sequences were listed in supplemental table 1.

Cortical stab injury

Adult male mice aged 3–4 months were used for all the experiments. Cortical stab injury was performed as described earlier (Auguste *et al*. 2007, Buffo *et al*. 2008, Robel *et al*. 2011a),

with slight modifications. Briefly, mice were anesthetized deeply with chloral hydrate at a dose of 400 mg/kg by intraperitoneal injection (Nacalai Tesque, Kyoto, Japan). A stab wound lesion was created with a scalpel blade by sagittal insertion through the skull to the right cerebral cortex at a depth of 1.0 mm, 1.7 mm lateral to the midline and 1.0–2.5 mm posterior to the bregma. The mice were sacrificed from 1 d to 7 d after the stab injury and subjected to the morphological and biochemical analyses described below.

Histological and immunohistochemical analyses

Brains were removed from the C57BL/6 mice after perfusion with 4% paraformaldehyde, and cortical sections (10-μm-thick sections) were cut on a cryostat. Sections were processed for Fluoro-Jade C staining (Millipore, Billerica, MA) or for immunostaining with antibodies against Ndrg2 (Santa Cruz Biotechnology, Dallas, TX), GFAP (Dako, Glostrup, Denmark; Sigma, St. Louis, MO), Iba1 (Wako, Osaka, Japan), NeuN (Millipore), nestin (Millipore), SRY-box containing gene 2 (Sox2) (Santa Cruz Biotechnology), single strand DNA (ssDNA) (Dako), and S100β (Sigma). Alexa488 (Invitrogen, Carlsbad, CA)- or Cy3-conjugated secondary antibody (Jackson ImmunoResearch Laboratories, West Grove, PA) were used for visualization of immunolabeling. Imaging was performed on a laser scanning confocal microscope (Eclipse TE2000U; Nikon, Tokyo, Japan) with the Nikon EZ-C1 software. The immunoreactivity of GFAP was quantified using Image J (version 1.42, Wayne Rasband, National Institutes of Health, Bethesda, Maryland, USA), and the number of Iba1-positive cells was counted in four 0.07-mm^2 rectangles stepwise from the center of the stab wound to a distance of 0.4 mm. The number of Fluoro-Jade C- or ssDNA-positive cells, and the number of GFAP- and IL-6-double positive cells were counted in 0.27-mm^2 rectangles at the center of the lesion.

Western blot and ELISA

Samples from mouse brains, including the stab wound lesion or the corresponding region in the contralateral side, and from cultured astrocytes were solubilized in buffer containing 10 mM Tris (pH 7.6), 1 mM EDTA, 150 mM NaCl, 1% NP-40, 0.1% SDS, 0.2% sodium deoxycholate, 1 mM PMSF, 1 μg/mL aprotinin, 10 mM NaF, and 1 mM Na_3VO_4. Western blot was performed using antibodies against Ndrg2, GFAP, HO-1 (Abcam, Cambridge, UK), phospho-STAT3 (Tyr705) (Cell Signaling Technology, Danvers, MA), STAT3 (Cell Signaling Technology), and β-actin (Sigma). Sites of primary antibody binding were determined by using an ECL system (GE Healthcare, Pittsburgh, PA) with horseradish peroxidase (HRP)-conjugated secondary antibodies (Santa Cruz Biotechnology). The intensity of each band was quantified using Image J (version 1.42). The IL-6 levels in the brain samples and the culture media of astrocytes were measured using an ELISA kit (eBioscience, San Diego, CA) following the manufacturer's instructions.

Quantitative real-time RT-PCR

Total RNA was extracted from cultured astrocytes and the contralateral or ipsilateral cortex after stab injury by using the RNeasy Lipid Tissue Mini Kit (Qiagen, Valencia, CA). cDNA was prepared using PrimeScript (Takara, Shiga, Japan) with 1 μg of total RNA. Each cDNA sample was amplified in a reaction mixture containing 1 unit of Taq DNA polymerase (Takara) and primers specific for *Ndrg2*. For quantitative analysis, cDNA was amplified with Thunderbird SYBR qPCR Mix (Toyobo, Osaka, Japan) by using primers specific for *Gfap*, *Hmox1* (heme oxygenase 1), *Serpina3n* (serine peptidase inhibitor clade A member 3), *Lcn2* (lipocalin 2), *Iba1*, *Cxcl1* (chemokine [C-X-C motif] ligand 1), *Ccl2* (chemokine [C-C motif] ligand 2), *Tnfa* (tumor necrosis factor α), *Lif* (leukemia-inhibitory factor), *Il6* (interleukin-6), *Cntf* (ciliary neurotrophic factor), *Tgfb1* (transforming growth factor β), *Edn1* (endothelin-1),

Ndrg2, *Atf3* (activating transcription factor 3) and *Ccnd1* (cyclin D1). The comparative Ct method was used for data analyses with MxPro 4.10 (Agilent Technologies, Santa Clara, CA). The expression levels for each gene were normalized to those of *Gapdh* (glyceraldehyde-3-phosphate dehydrogenase) or *Actb* (β-actin). Primer sequences were listed in supplemental table 1.

Recombinant adenovirus

Recombinant adenovirus AxCALNLZ2 Ndrg2 (AdV-Ndrg2) expressing FLAG (DYKDDDK)-tagged Ndrg2 under the control of Cre-recombinase was developed as described before (Takeichi *et al*. 2011), and adenovirus was amplified in HEK293 cells. Viral titers were determined by the tissue culture infectious dose method ($TCID_{50}$) in HEK 293 cells. Viral stocks had titers of ~1 × 10^8 PFU/mL. Cre-recombinase–expressing adenovirus AxCANCre and the control virus AxCALNLZ2 LacZ (AdV-LacZ) were obtained from Takara.

Cell culture

Astrocytes were isolated from cerebral cortex of 1- to 3-d-old neonatal mice following a previously described method with minor modifications (Kuwabara *et al*. 1996). Briefly, cerebral hemispheres were harvested from neonatal mice, and the meninges were carefully removed. Brain tissue was then digested at 37ºC in HEPES-buffered saline (HBS) containing Dispase II (2 mg/mL). Cells were collected by centrifugation and resuspended in minimum essential medium (MEM) supplemented with 10% fetal bovine serum (FBS). After 10-d cultivation, microglial cells were removed by aspiration after shaking and the adherent cell population was collected and used for experiments. When the cultures achieved confluence, cells were incubated in serum-free medium overnight and then treated with several astroglial

activators such as forskolin (10 μM; Wako, Osaka, Japan), ATP (1 mM; Sigma), LPS (1 μg/mL; Sigma), endothelin-1 (200 nM; Sigma), and TGFβ (25 ng/mL; Peprotech Inc. London, UK) in serum-free medium for indicated time. In some cases, cells were co-infected with Cre-expressing adenovirus and either Ndrg2-expressing adenovirus (AdV-Ndrg2) or a control adenovirus (AdV-LacZ), in which gene expression was controlled by the Cre-loxP system. Two days after adenovirus infection, the cells were incubated in the presence or absence of 10 μM forskolin for 8 h in serum-free medium. Total RNA and culture media were subjected to quantitative real-time RT-PCR (qRT-PCR) and ELISA, respectively.

3-(4, 5-Dimethyl-2-thiazolyl)-2,5-diphenyl tetrazolium bromide assay

Cell proliferation analysis was performed by the 3-(4, 5-Dimethyl-2-thiazolyl)-2,5-diphenyltetrazolium bromide (MTT) reduction assay to assess the mitochondrial activity at every 24 h up to 5 d after plating. Astrocytes isolated from WT or *Ndrg2*$^{-/-}$ mice were incubated with 0.5 mg/mL MTT (Nacalai Tesque) for 1 h at 37ºC. After aspiration of the MTT solution, the formazan crystals were dissolved in dimethyl sulfoxide. The absorbance of the dissolved solution was measured at a wavelength of 590 nm.

Scratch wound assay

Confluent monolayers of astrocytes were wounded by scratching with a sterile plastic 10 μL tip from left side to right side of the well (Robel *et al.* 2011a). Culture medium were immediately changed to remove the cell debris. Images were taken 24 h and immediately after medium change with using light microscope. The wound area was measured using ImageJ software, as described above.

Luciferase assay

Cultured astrocytes were co-transfected with cAMP-response element (CRE)- luciferase reporter plasmid (Stratagene) and control plasmid pRL-SV40 Renilla luciferase (Promega) using Lipofectamine 2000 (Invitrogen) as the transfection agent. Cells were incubated in serum-free medium overnight and then treated with forskolin at 10 μM for 6 h. The dual luciferase assay was performed according to the manufacturer's protocol (Promega). For each samples, the firefly luciferase activity (CRE-Luc) was normalized by reference to renilla luciferase activity (pRL-SV40).

Statistical analysis

All the results have been expressed in terms of mean ± standard error of the mean (S.E.M.), and statistical significance was determined by two-tailed and unpaired Student's *t*-tests or one-way analysis of variance (ANOVA) with the Bonferroni/Dunnett post-hoc test.

Results

Elevated expression of Ndrg2 and GFAP in the injured cerebral cortex

Consistent with our previous report (Takeichi *et al*. 2011), Ndrg2 was expressed selectively in astrocytes in the normal cerebral cortex (Supplemental Fig. 1A). To investigate the expression of Ndrg2 in the course of reactive astrogliosis, we used a mouse cortical stab injury model, which is a well-established model of acute brain injury (Auguste *et al*. 2007, Buffo *et al*. 2008, Robel *et al*. 2011a). Immunohistochemical analysis revealed that expression of GFAP, which is a marker of reactive astrocytes, began to elevate at day 1 after injury in fine processes of astrocytes and further increased at day 4 after injury in hypertrophic astrocytes around the lesion (Fig. 1A). It was rarely seen in the contralateral cortex with the exception in the surface of region. Western blot analysis revealed that expression of Ndrg2 protein was significantly higher in the ipsilateral side than that in the contralateral side, as early as day 1 after injury, in which significant GFAP induction did not occur yet (Fig. 1B). Immunohistochemical analysis also indicated high levels of Ndrg2 expression in the ipsilateral side, compared with the contralateral side at day 1 after injury in the both GFAP-positive and GFAP-negative cells around the lesion (Fig. 1C and Supplemental Fig. 1B). At day 4, most of the Ndrg2-expressing cells were co-labeled with GFAP, but not with NeuN or Iba1, the latter two are neuronal and microglial cell markers, respectively (Fig. 1D). Some of the Ndrg2-expressing cells in the injured cortex were co-labeled with nestin (Fig. 1D), which is a marker for progenitor cells and also reported to be expressed in reactive astrocytes (Buffo *et al*. 2008, Robel *et al*. 2011b, Shimada *et al*. 2012). These data indicate that expression of Ndrg2 is selectively observed in astrocytes, and its enhancement precedes that of GFAP after cotrical stab injury.

Generation of Ndrg2-deficient mice

To investigate the role of Ndrg2 *in vivo*, we generated *Ndrg2* knockout mouse using homologous recombination and the Cre/loxP system. As shown in Fig. 2A, *Ndrg2* was targeted with loxP-flanking sequences containing exons 3 and 4 of *Ndrg2*. Successful targeting was confirmed by Southern blot analysis (Fig. 2B). Then, *Ndrg2*$^{neo/+}$ mice were crossed with CAG-Cre transgenic mice to generate *Ndrg2*$^{+/-}$ mice. *Ndrg2*$^{-/-}$ mice grew normally and were fertile. Disruption of Ndrg2 was confirmed in several tissues such as the brain, liver and heart at both mRNA and protein levels by RT-PCR and western blot analysis, respectively (Fig. 2C and D).

Impaired glial response in Ndrg2-deficient mice after stab injury

To study the effect of Ndrg2 deletion after brain injury, WT and *Ndrg2*$^{-/-}$ mice received a cortical stab injury. In WT mice, the stab injury markedly increased the mRNA expression of the following genes, which started to increase at day 1 and peaked at day 4 after injury (Fig. 3A and supplemental Fig. 2A): reactive astroglial markers such as *Gfap*, *Serpna3n*, and *Lcn2* (Naudé *et al*. 2012, Zamanian *et al*. 2012); the microglial marker *Iba1*; the antioxidative gene *Hmox1* known as HO-1 (Park *et al*. 2008, Hashida *et al*. 2012); and inflammatory mediators such as *Cxcl1, Ccl2* and *Tnfa*. In *Ndrg2*$^{-/-}$ mice, the levels of mRNA expression of these genes were significantly lower than those of WT mice at day 1 and/or day 4 after stab injury (Fig. 3A). Consistent with these results, the levels of protein expression of GFAP, Iba1 and HO-1 were significantly lower in *Ndrg2*$^{-/-}$ mice at day 4 after stab injury (Fig. 3B and Supplemental Fig. 2E). Similarly, immunohistochemical analysis showed that the intensity of the GFAP signal was significantly lower in *Ndrg2*$^{-/-}$ mice than in WT mice in all the regions within 400 μm from the injury site (Fig. 3C). In contrast, the number of Iba1-positive microglia was significantly lower in *Ndrg2*$^{-/-}$ mice in the regions closer to the injury site (Fig. 3C). Taken together with the

fact that Ndrg2 is expressed in astrocytes, reduced levels of microglial accumulation in *Ndrg2*$^{-/-}$ mice after stab injury may be a secondary effect of impaired astroglial activation.

Impaired IL-6/STAT3 signaling in Ndrg2-deficient mice

To investigate whether impaired astroglial activation in *Ndrg2*$^{-/-}$mice occurs at early periods after stab injury, the expression of several astroglial activators such as IL-6 family cytokines, including *Il6*, *Lif* and *Cntf*, and other soluble factors such as *Tgfβ* and *Edn1* were analyzed by qRT-PCR. Cortical stab injury strongly induced *Il6* and *Lif* at day 1 and *Cntf* at day 4 after stab injury in WT mice, but the induction was significantly reduced in *Ndrg2*$^{-/-}$ mice (Fig. 4A). In our model, *Tgfb1* or *Edn1* was not significantly induced in both genotypes (Supplemental Fig. 2B). Consistent with these results, immunohistochemical analysis revealed that IL-6-positive astrocytes were observed more often in the lesion site of WT mice than *Ndrg2*$^{-/-}$ mice at day 1 after injury (Fig. 4B). Additionally, there was a tendency for decrease in the level of IL-6 protein, which was examined by ELISA; the level was lower in *Ndrg2*$^{-/-}$ mice than in WT mice after stab injury (Supplemental Fig. 2D; 37.4 pg/mL in the ipsilateral side and 16.8 pg/mL in the contralateral side in WT mice, and 24.4 pg/mL in the ipsilateral side and 17.1 pg/mL in the contralateral side in *Ndrg2*$^{-/-}$ mice). Next, the status of IL-6 signaling was studied. The binding of IL-6 family cytokines to their receptors triggers the activation of STAT3, which has been reported to play a critical role in astrogliosis (Okada *et al*. 2006, Hermann *et al*. 2008). Cortical stab injury induced phosphorylation of STAT3 at tyrosine 705 in WT mice to a level significantly higher than that in *Ndrg2*$^{-/-}$ mice (Fig. 4C).

Attenuated response in Ndrg2-deficient astrocytes after forskolin stimulation

To examine whether the impaired glial response in *Ndrg2*$^{-/-}$ mice was the effect of Ndrg2 deficiency in astrocytes, we employed primary astroglial cultures derived from WT and

Ndrg2$^{-/-}$ mice. In cultured astrocytes, there was no difference in proliferation and migration between both genotypes determined by MTT reduction assay and scratch wound assay, respectively (Fig. 5A and B). In the latter assay in WT astrocytes, there was no significant difference in the expression of *Ndrg2*, *Il6* or *Gfap* (Supplemental Fig. 3A and B). Next, astrocytes were stimulated by the several reagents known to induce astroglial activation *in vitro* and/or *in vivo* (Gadea *et al*. 2008, Sofroniew 2009, Schachtrup *et al*. 2010). Western blot analysis revealed that the expression of Ndrg2 was enhanced most by forskolin treatment among the reagents tested (Fig. 5C, D and E). Consistent with the results *in vivo*, the level of induction of *Il6* and *Gfap* was significantly lower in *Ndrg2*$^{-/-}$ astrocytes 8 h and 24 h after forskolin treatment, respectively, although the CRE reporter activity was somehow increased at 6 h (Fig. 5F, G and H). To investigate whether downregulation of IL-6 expression was caused by the deletion of Ndrg2, re-expression of Ndrg2 in *Ndrg2*$^{-/-}$ astrocytes was carried out by the infection of Ndrg2-expressing adenovirus. The expression levels of Ndrg2 were determined by qRT-PCR and western blot (Fig. 5I and J). The reduced level of IL-6 expression in *Ndrg2*$^{-/-}$ astrocytes was completely restored by adenovirus-mediated Ndrg2 expression at both mRNA and protein levels (Fig. 5K and L), while the restoration in *Gfap* expression was milder (Supplemental Fig. 3C). These results suggest that the Ndrg2 positively regulates IL-6 expression in astrocytes.

Attenuated neuronal death in Ndrg2$^{-/-}$ *mice after cortical stab injury*

To evaluate the neuronal damage in *Ndrg2*$^{-/-}$ mice after stab injury, histological and immunohistochemical analyses were performed at day 4 after lesion. Both Fluoro-Jade C staining and ssDNA immunostaining, which detect apoptotic cells and degenerating neurons, respectively, revealed that *Ndrg2*$^{-/-}$ mice exhibited significantly less damage in the wounded area than WT mice (Fig. 6A). Most of the cells positive for ssDNA in their nuclei were also

positive for Fluoro-Jade C in both genotypes (WT: 97.5%, *Ndrg2*$^{-/-}$ mice: 97.8%). Consistent with this finding, qRT-PCR revealed that the induction level of *Atf3*, which is known to increase in response to neuronal injury (van der Weerd *et al*. 2010, Zhang *et al*. 2011), was significantly reduced in *Ndrg2*$^{-/-}$ mice (Fig. 6B). These results indicated that Ndrg2 deletion leads to reduction of neuronal death after cortical stab injury.

Discussion

In this study, we demonstrated that Ndrg2 plays an important role in the positive regulation of early reactive astrogliosis, at least in part, through the activation of IL-6/STAT3 signaling after cortical stab injury. Additionally, the deletion of Ndrg2 resulted in the attenuated recruitment of microglia to the lesion site and prevented neuronal death. To our knowledge, this is the first report clarifying the role of Ndrg2 in pathological conditions *in vivo* by using *Ndrg2*-deficient mice.

Reactive astrogliosis is not an all-or-none response but is a graded spectrum of molecular changes associated with cellular hypertrophy, proliferation, and glial scar formation (Sofroniew and Vinters 2010). It is accompanied by the up-regulation of intermediate filament proteins including GFAP. Important finding in this study is that Ndrg2 is an early injury-responsive gene in astrocytes. Upregulation of Ndrg2 was observed at day 1 after injury, in which that of GFAP was partially obserbed by immunohistochemical analysis (Fig. 1A, B, C and Fig. 3B). Furthermore, we demonstrated that the induction of reactive astroglial markers, such as GFAP, *Serpina3n*, and *Lcn2* (Fig. 3A and B), and cellular hypertrophy (Fig. 3C) were significantly lower in *Ndrg2*$^{-/-}$ mice than in WT mice after cortical stab injury. These observations are consistent with our previous report describing the role of Ndrg2 in the morphological changes in cultured astrocytes (Takeichi *et al*. 2011). In contrast, the effect of Ndrg2 on cell proliferation during astrogliosis was not clear in this study. Previous studies from our and other groups demonstrated the inhibitory role of Ndrg2 on cell proliferation in different tumor cells and in astrocytes (Deng *et al*. 2003, Kim *et al*. 2009, Takeichi *et al*. 2011). There may be a couple of explanations for this discrepancy. One is the functional redundancy of Ndrg2 in the astroglial proliferation. In most of the previous reports, Ndrg2 was transiently silenced at mRNA level (Foletta *et al*. 2009) or inactivated at the protein level by overexpressing mutant proteins (Kim *et al*. 2009), while Ndrg2 was genetically deleted from

the developmental/embryonic stages in this study. This may cause altered gene expression by complementary mechanisms. Another explanation is that the cortical stab injury used in this study was relatively mild and may not cause high levels of astroglial proliferation. In this regard, the induction of *Ccnd1,* a gene that encodes CyclinD1, a marker of cell cycle progression in G1/S phase, was very mild (less than 2-fold increase in both genotypes) after stab injury (Supplemental Fig. 2C).

Among the triggering signals for astrogliosis that were investigated in this study, IL-6 was the most active molecule after stab injury. Activation of IL-6/STAT3 signaling in the injured CNS has been reported to induce strong astrogliosis. Loss of STAT3 or suppressor of cytokine signaling 3 (SOCS3), a negative feedback molecule of STAT3, in mice under the control of GFAP or the nestin promoter has been reported to reduce or enhance reactive astrogliosis, respectively, in a spinal cord injury model (Okada *et al*. 2006, Hermann *et al*. 2008). In this study, the effect of Ndrg2 deletion on IL-6 expression was observed to a larger extent in mouse brains (Fig. 4A) than in cultured astrocytes (Fig. 5G), suggesting that Ndrg2 may promote IL-6 expression through both a cell-autonomous mechanism in astrocytes and a non-cell autonomous mechanism through other type of cells including microglia. Consistent with this, not only reactive astrogliosis but also microglial accumulation was impaired in *Ndrg2*$^{-/-}$ mice after stab injury (Fig. 3A and C), as previously reported in *Il6*$^{-/-}$ mice after cortical freeze injury (Penkowa *et al*. 2000). Ndrg2 may contribute to a positive feedback loop for IL-6 signaling, which is referred to as IL-6 amplifier activation (Murakami and Hirano 2012).

Although *Il6*$^{-/-}$, *GFAP-Stat3*$^{-/-}$, *Nestin-Stat3*$^{-/-}$ and *Ndrg2*$^{-/-}$ mice demonstrated similar phenotypes in reactive astrogliosis, they demonstrated different phenotypes in neurons. Neuronal damage was exaggerated in the first 3 types of mice (Penkowa *et al*. 2000, Okada *et al*. 2006, Herrmann *et al*. 2008), while it was attenuated in *Ndrg2*$^{-/-}$ mice (Fig. 6). This discrepancy could be attributed to the difference of the severity of the insult or to the

inflammatory response in each pathological model. In this regard, it is noteworthy that the expression level of chemokines and activation of microglia were reduced in *Ndrg2*$^{-/-}$ mice. Furthermore, induction of *Lcn2* (lipocalin-2), a chemokine inducer released from reactive astrocytes and promotes neuronal death (Bi *et al*. 2013), was reduced after stab injury in *Ndrg2*$^{-/-}$ mice (Fig. 3A). Although it is still controversial whether astrogliosis is beneficial or detrimental, *Ndrg2*$^{-/-}$ mice will be a useful tool for studying the effect of glial activation on the neuronal survival/activity in different disease models.

It has been reported that Ndrg2 is upregulated by adrenal steroid hormones (Nichols 2003), which occurs through the glucocorticoid receptor but not through the glucocorticoid response element half-site (GRE1/2) (Takahashi *et al*. 2005b). In the current cortical stab injury model, Ndrg2 might be upregulated through the stress-associated steroid hormones or some stress-associated signals, including protein kinase A, as described in cultured astrocytes in this study (Fig. 5C and D). Further studies are required for clarifying the molecular mechanism underlying the regulation of Ndrg2 expression.

In conclusion, the current study demonstrated that Ndrg2 is an injury-responsive gene that is involved in the early phase of astroglial activation and that it positively regulates reactive astrogliosis and the subsequent inflammatory response, at least in part, through the activation of IL-6/STAT3 signaling. Thus, Ndrg2 could be a new therapeutic target in various neurological conditions related to astroglial activation and inflammation.

Acknowledgements

The authors declare no conflict of interest. This work was supported by a Grant-in-Aid for young scientists (B) (23790219) from Japanese Society for the Promotion of Science.

We thank Ms. Yoko Esaki and Ms. Kiyo Kawata (NPO Biotechnology Research and Development) for their efforts in the generation of Ndrg2 chimeric mice. The CAG-Cre mice

were kindly provided by Dr. Junichi Miyazaki (Osaka University). We are grateful to Ms. Nahoko Okitani, Mr. Takashi Tamatani, and Ms. Michiyo Tamatani for technical assistance.

References

Araque, A., Parpura, V., Sanzgiri, R. P., Haydon, P. G. (1999) Tripartite synapses: glia, the unacknowledged partner. *Trends Neurosci.* **22**, 208-215

Auguste, K. I., Jin, S., Uchida, K., Yan, D., Manley, G. T., Papadopoulos, M. C., Verkman, A. S. (2007) Greatly impaired migration of implanted aquaporin-4-deficient astroglial cells in mouse brain toward a site of injury. *FASEB J.* **21**, 108-116

Bi F., Huang C., Tong J., Qiu G., Huang B., Wu Q., Li F., Xu Z., Bowser R., Xia X. G., Zhou H. (2013) Reactive astrocytes secrete lcn2 to promote neuron death. *Proc. Natl. Acad. Sci. USA.* **110**, 4069-4074.

Boulkroun, S., Fay, M., Zennaro, M. C., Escoubet, B., Jaisser, F., Blot-Chabaud, M., Farman, N., Courtois-Coutry, N. (2002) Characterization of rat NDRG2 (N-Myc downstream regulated gene 2), a novel early mineralocorticoid-specific induced gene. *J. Biol. Chem.* **277**, 31506-31515

Brambilla, R., Bracchi-Ricard, V., Hu, W. H., Frydel, B., Bramwell, A., Karmally, S., Green, E. J., Bethea, J. R. (2005) Inhibition of astroglial nuclear factor kappaB reduces inflammation and improves functional recovery after spinal cord injury. *J. Exp. Med.* **202**, 145-156

Buffo, A., Rite, I., Tripathi, P., Lepier, A., Colak, D., Horn, A. P., Mori, T., Götz, M. (2008) Origin and progeny of reactive gliosis: A source of multipotent cells in the injured brain. *Proc. Natl. Acad. Sci. USA* **105**, 3581-3586

Deng, Y., Yao, L., Chau, L., Ng, S. S., Peng, Y., Liu, X., Au, W. S., Wang, J., Li, F., Ji, S., Han, H., Nie, X., Li, Q., Kung, H. F., Leung, S. Y., Lin, M. C. (2003) N-Myc downstream-regulated gene 2 (NDRG2) inhibits glioblastoma cell proliferation. *Int. J. Cancer* **106**, 342-347

Foletta, V. C., Prior, M. J., Stupka, N., Carey, K., Segal, D. H., Jones, S., Swinton, C., Martin, S., Cameron-Smith, D., Walder, K. R. (2009) NDRG2, a novel regulator of myoblast proliferation, is regulated by anabolic and catabolic factors. *J. Physiol.* **1**, 1619-1634

Gadea, A., Schinelli, S., Gallo, V. (2008) Endothelin-1 regulates astrocyte proliferation and reactive gliosis via a JNK/c-Jun signaling pathway. *J. Neurosci.* **28**, 2394-2408.

Hashida, K., Kitao, Y., Sudo, H., Awa, Y., Maeda, S., Mori, K., Takahashi, R., Iinuma, M., Hori, O. (2012) ATF6alpha promotes astroglial activation and neuronal survival in a chronic mouse model of Parkinson's disease. *PLoS One* **7**, e47950

Herrmann, J. E., Imura, T., Song, B., Qi, J., Ao, Y., Nguyen, T. K., Korsak, R. A., Takeda, K., Akira, S., Sofroniew, M. V. (2008) STAT3 is a critical regulator of astrogliosis and scar formation after spinal cord injury. *J. Neurosci.* **28**, 7231-7243

Huang, C., Han, X., Li, X., Lam, E., Peng, W., Lou, N., Torres, A., Yang, M., Garre, J. M., Tian, G. F., Bennett, M. V., Nedergaard, M., Takano, T. (2012) Critical role of connexin 43 in secondary expansion of traumatic spinal cord injury. *J. Neurosci.* **32**, 3333-3338

Hwang, J., Kim, Y., Kang, H. B., Jaroszewski, L., Deacon, A. M., Lee, H., Choi, W. C., Kim, K. J., Kim, C. H., Kang, B. S., Lee, J. O., Oh, T. K., Kim, J. W., Wilson, I. A., Kim, M. H. (2011) Crystal structure of the human N-Myc downstream-regulated gene 2 protein provides insight into its role as a tumor suppressor. *J. Biol. Chem.* **286**, 12450-12460

Iadecola, C., Nedergaard, M. (2007) Glial regulation of the cerebral microvasculature. *Nat. Neurosci.* **10**, 1369-1376

Jeschke, J., Van, Neste, L., Glöckner, S. C., Dhir, M., Calmon, M. F., Deregowski, V., Van, Criekinge, W., Vlassenbroeck, I., Koch, A., Chan, T. A., Cope, L., Hooker, C. M., Schuebel, K. E., Gabrielson, E., Winterpacht, A., Baylin, S. B., Herman, J. G., Ahuja, N. (2012) Biomarkers for detection and prognosis of breast cancer identified by a functional hypermethylome screen. *Epigenetics* **7**, 701-709

Kim, A., Kim, M. J., Yang, Y., Kim, J. W., Yeom, Y. I., Lim, J. S. (2009) Suppression of NF-kappaB activity by NDRG2 expression attenuates the invasive potential of highly malignant tumor cells. *Carcinogenesis* **30**, 927-936

Kim, Y. J., Yoon, S. Y., Kim, J. T., Choi, S. C., Lim, J. S., Kim, J. H., Song, E. Y., Lee, H. G., Choi, I., Kim, J. W. (2009) NDRG2 suppresses cell proliferation through down-regulation of AP-1 activity in human colon carcinoma cells. *Int. J. Cancer* **124**, 7-15

Kuwabara, K., Matsumoto, M., Ikeda, Jun., Hori, O., Ogawa, S., Maeda, Y., Kitagawa, K., Imuta, N., Kinoshita, T., Stern, D. M., Yanagi, H., Kamada, T. (1996) Purification and characterization of a novel stress protein, the150-kDa oxygen-regulated protein (ORP150), from cultured rat astrocytes and its expression in ischemic mouse brain. *J. Biol. Chem.* **271**, 5025-5032 Murakami, M., Hirano, T. (2012) The pathological and physiological roles of IL-6 amplifier activation. *Int. J. Biol. Sci.* **8**, 1267-1280.

Li, Y., Shen, L., Cai, L., Wang, Q., Hou, W., Wang, F., Zeng, Y., Zhao, G., Yao, L., Xiong, L. (2011) Spatial-temporal expression of NDRG2 in rat brain after focal cerebral ischemia and reperfusion. *Brain Res.* **1382**, 252-258

Lusis, E. A., Watson, M. A., Chicoine, M. R., Lyman, M., Roerig, P., Reifenberger, G., Gutmann, D. H., Perry, A. (2005) Integrative genomic analysis identifies NDRG2 as a candidate tumor suppressor gene frequently inactivated in clinically aggressive meningioma. *Cancer Res.* **65**, 7121-7126

Mitchelmore, C., Büchmann-Møller, S., Rask, L., West, M. J., Troncoso, J. C., Jensen, N. A. (2004) NDRG2: a novel Alzheimer's disease associated protein. *Neurobiol. Dis.* **16**, 48-58

Murray, J. T., Campbell, D. G., Morrice, N., Auld, G. C., Shpiro, N., Marquez, R., Peggie, M., Bain, J., Bloomberg, G. B., Grahammer, F., Lang, F., Wulff, P., Kuhl, D., Cohen, P. (2004) Exploitation of KESTREL to identify NDRG family members as physiological substrates for SGK1 and GSK3. *Biochem. J.* **384**, 477-488

Naudé, P. J., Nyakas, C., Eiden, L. E., Ait-Ali, D., van, der, Heide, R., Engelborghs, S., Luiten, P. G., De, Deyn, P. P., den, Boer, J. A., Eisel, U. L. (2012) Lipocalin 2: novel component of proinflammatory signaling in Alzheimer's disease. *FASEB J.* **26**, 2811-2823

Nichols, N. R. (2003) Ndrg2, a novel gene regulated by adrenal steroids and antidepressants, is highly expressed in astrocytes. *Ann. N. Y. Acad. Sc.* **1007**, 349-356

Okada, S., Nakamura, M., Katoh, H., Miyao, T., Shimazaki, T., Ishii, K., Yamane, J., Yoshimura, A., Iwamoto, Y., Toyama, Y., Okano, H. (2006) Conditional ablation of Stat3 orSocs3 discloses a dual role for reactive astrocytes after spinal cord injury. *Nat. Med.* **12**, 829-834

Okuda, T., Kokame, K., Miyata, T. (2008) Differential expression patterns of NDRG family proteins in the central nervous system. *J. Histochem. Cytochem.* **56**, 175-182Schummers, J., Yu, H., Sur, M. (2008) Tuned responses of astrocytes and their influence on hemodynamic signals in the visual cortex. *Science* **320**, 1638-1643

Park, C., Cho, I. H., Kim, D., Jo, E. K., Choi, S. Y., Oh, S. B., Park, K., Kim, J. S., Lee, S. J. (2008) Toll-like receptor 2 contributes to glial cell activation and heme oxygenase-1 expression in traumatic brain injury. *Neurosci. Lett.* **431**, 123-128

Penkowa, M., Giralt, M., Carrasco, J., Hadberg, H., Hidalgo, J. (2000) Impaired inflammatory response and increased oxidative stress and neurodegeneration after brain injury in interleukin-6-deficient mice. *Glia* **32**, 271-285

Qu, X., Zhai, Y., Wei, H., Zhang, C., Xing, G., Yu, Y., He, F. (2002) Characterization and expression of three novel differentiation-related genes belong to the human NDRG gene family. *Mol. Cell. Biochem.* **229**, 35-44

Robel, S., Bardehle, S., Lepier, A., Brakebusch, C., Götz, M. (2011a) Genetic deletion of cdc42 reveals a crucial role for astrocyte recruitment to the injury site in vitro and in vivo. *J. Neurosci.* **31**, 12471-12482

Robel, S., Berninger, B., Götz, M. (2011b) The stem cell potential of glia: lessons from reactive gliosis. *Nat. Rev. Neurosci.* **12**, 88-104

Sasaki, K., Miyazaki, J. (1997) A transgenic mouse line that retains Cre recombinase activity in mature oocytes irrespective of the cre transgene transmission. *Biochem. Biophys. Res. Commun.* **237**, 318-324

Schachtrup, C., Ryu, J. K., Helmrick, M. J., Vagena, E., Galanakis, D. K., Degen, J. L., Margolis, R. U., Akassoglou, K. (2010) Fibrinogen triggers astrocyte scar formation by promoting the availability of active TGF-beta after vascular damage. *J. Neurosci.* **30**, 5843-5854

Shimada, I. S., LeComte, M. D., Granger, J. C., Quinlan N. J., Spees, J. L. (2012) Self-renewal and differentiation of reactive astrocyte-derived neural stem/progenitor cells isolated from the cortical peri-infarct area after stroke. *J. Neurosci.* **32**, 7926-7940

Silver, J., Miller, J. H. (2004) Regeneration beyond the glial scar. *Nat. Rev. Neurosci.* **5**, 146-156

Sofroniew, M. V. (2009) Molecular dissection of reactive astrogliosis and glial scar formation. *Trends Neurosci.* **32**, 638-647

Sofroniew, M. V., Vinters, H. V. (2010) Astrocytes: biology and pathology. *Acta. Neuropathol.* **119**, 7-35

Sung, B., Lim, G., Mao, J. (2003) Altered expression and uptake activity of spinal glutamate transporters after nerve injury contribute to the pathogenesis of neuropathic pain in rats. *J. Neurosci.* **23**, 2899-2910

Takahashi, K., Yamada, M., Ohata, H., Momose, K., Higuchi, T., Honda, K., Yamada, M. (2005a) Expression of Ndrg2 in the rat frontal cortex after antidepressant and electroconvulsive treatment. *Int. J. Neuropsychopharmacol.* **8**, 381-389 (2005a)

Takahashi, K., Yamada, M., Ohata, H., Honda, K., Yamada, M. (2005b) Ndrg2 promotes neurite outgrowth of NGF-differentiated PC12 cells. *Neurosci. Lett.* **388**, 157-162

Takeichi, T., Takarada-Iemata, M., Hashida, K., Sudo, H., Okuda, T., Kokame, K., Hatano, T., Takanashi, M., Funabe, S., Hattori, N., Kitamura, O., Kitao, Y., Hori, O. (2011) The effect of Ndrg2 expression on astroglial activation. *Neurochem. Int.* **59**, 21-27

van der Weerd, L., Tariq, Akbar, M., Aron, Badin, R., Valentim, L. M., Thomas, D. L., Wells, D. J., Latchman, D. S., Gadian, D. G., Lythgoe, M. F., de Belleroche, J. S. (2010) Overexpression of heat shock protein 27 reduces cortical damage after cerebral ischemia. *J. Cereb. Blood Flow Metab.* **30**, 849-856

Widestrand, A., Faijerson, J., Wilhelmsson, U., Smith, P. L., Li, L., Sihlbom, C., Eriksson, P. S., Pekny, M. (2007) Increased neurogenesis and astrogenesis from neural progenitor cells grafted in the hippocampus of GFAP-/- Vim-/- mice. *Stem Cells* **25**, 2619-2627

Zamanian, J. L., Xu, L., Foo, L. C., Nouri, N., Zhou, L., Giffard, R. G., Barres, B. A. (2012) Genomic analysis of reactive astrogliosis. *J. Neurosci.* **32**, 6391-6410

Zhang, S. J., Buchthal, B., Lau, D., Hayer, S., Dick, O., Schwaninger, M., Veltkamp, R., Zou, M., Weiss, U., Bading, H. (2011) A signaling cascade of nuclear calcium-CREB-ATF3 activated by synaptic NMDA receptors defines a gene repression module that protects

against extrasynaptic NMDA receptor-induced neuronal cell death and ischemic brain damage. *J. Neurosci.* **31**, 4978-4990

Zhu, H., Zhao, J., Zhou, W., Li, H., Zhou, R., Zhang, L., Zhao, H., Cao, J., Zhu, X., Hu, H., Ma, G., He, L., Yao, Z., Yao, L., Guo, X. (2012) Ndrg2 regulates vertebral specification in differentiating somites. *Dev. Biol.* **369**, 308-318

Figure legends

Figure 1. Increased Ndrg2 expression in astrocytes after cortical stab injury.

(A) GFAP immunostaining was performed using brain sections obtained at day 1 and day 4 after cortical stab injury. The ipsilateral (ipsi) and the contralateral (contra) areas are presented. *Dotted lines* indicate the stab wounds. *Enlarged picture* indicates a single GFAP-positive astrocyte. *Scale bars* = 100 μm. (B) Ndrg2 and GFAP protein expression from day 1 to day 7 after cortical stab injury. Protein extracts from the lesion site (ipsi: ipsilateral) and control side (c: contralateral) were subjected to western blot analysis. Quantified data are presented in the *right graph*. Data are shown as mean ± SEM (n = 3–5). *P < 0.05, **P < 0.01 *versus* the contralateral cortex. (C) Ndrg2 (*red*) and GFAP (*green*) immunostaining was performed using brain sections obtained at day 1 after injury. The ipsilateral and the contralateral areas are presented. High magnification of framed area is shown in the *enlarged picture*. *Dotted lines* indicate the stab wounds. *Scale bars* = 50 μm. (D) Immunostaining for Ndrg2 (*red*) and cellular markers (*green*) including GFAP, Iba1, NeuN and nestin, was performed using brain sections obtained at day 4 after injury. *Scale bars* = 50 μm.

Figure 2. Targeted disruption of *Ndrg2*.

(A) Schematic representation of the WT *Ndrg2* locus, targeting vector, targeted allele, and deleted allele. The targeting vector replaces the coding region of exons 3 and 4 with loxP-flanked exons 3 and 4. Neomycin-resistance cassette was removed in the CRE-deleted allele. (B) Southern blot-based analysis of genomic DNA isolated from the WT ES cells (+/+) and the *Ndrg2*-targeted ES cells (+/neo). Targeted allele was confirmed by 2 different probes that recognize the 5′ site and 3′ site of fragments digested with *Eco*T221 and *Dra*I, respectively.

(C) PCR analysis and (D) western blot analysis showing deletion of Ndrg2 in the brain, liver, and heart from mice homozygous for the *Ndrg2*-deleted allele.

Figure 3. Glial response after cortical stab injury in *Ndrg2*-deficient mice

(A) Temporal gene expression profile for gliosis markers and chemokines after stab injury. Total RNA prepared from the ipsilateral (ipsi) and contralateral (c) cortices of WT mice and *Ndrg2*$^{-/-}$ mice from day 1 to day 7 after injury were subjected to quantitative RT-PCR using primers specific for *Gfap*, *Hmox1*, *Serpina3n*, *Lcn2*, *Iba1*, and *Ccl2*. Data are shown as mean ± SEM (n = 3–4). *P < 0.05, **P < 0.01 *versus* each contralateral cortex. $^{\#}$P < 0.05, $^{\#\#}$P < 0.01 *versus* indicated conditions. (B) Protein expression of GFAP and HO-1 from day 1 to day 7 after cortical stab injury. Protein extracts from the ipsilateral (ipsi) and contralateral (c) cortices of WT mice and *Ndrg2*$^{-/-}$ mice were used for western blot analysis. Quantified data are presented in the *right graphs*. Data are shown as mean ± SEM (n = 3–5). $^{\#}$P < 0.05 *versus* indicated conditions. (C) Brain sections were prepared from WT mice and *Ndrg2*$^{-/-}$ mice at day 4 after cortical stab injury and subjected to immunostaining for GFAP (*red*) and Iba1 (*green*). *Lower panels* represent high magnification of the white box in the *upper panels*. *Enlarged picture* in *lower panels* indicates a representative single GFAP-positive astrocyte. *Dotted lines* indicate the stab wound. *Scale bars* = 200 μm (*upper panel*), 50 μm (*lower panel*). Quantified intensity of GFAP immunostaining and cell numbers of Iba1-positive cells are presented in the *right graphs*. Data are shown as mean ± SEM (n = 6). #P < 0.05, ##P < 0.01 *versus* indicated conditions.

Figure 4. IL-6/STAT3 signaling in *Ndrg2*-deficient mice.

(A) Temporal gene expression profile for astroglial activators after stab injury. Total RNA was extracted from ipsilateral and contralateral cortices from day 1 to day 7 after injury and

subjected to qRT-PCR using primers specific for *Il6*, *Lif*, and *Cntf*. Data are shown as mean ± SEM (n = 3-4). *P < 0.05 *versus* indicated conditions. (B) Brain sections were prepared at day 1 after stab injury and subjected to immunostaining for GFAP (*green*) and IL-6 (*red*). GFAP and IL-6 double-positive cells in the white box are enlarged in the *lower panels*. *Scale bars* = 20 μm (*upper panel*), 10 μm (*lower panel*). Quantified data are presented in the *right graph*. Data are shown as mean ± SEM (n = 5). *P < 0.05 *versus* WT mice. (C) Phosphorylation of STAT3 at day 1 after stab injury. Protein extracts from the ipsilateral (ipsi) and contralateral (c) cortices of WT and *Ndrg2*$^{-/-}$ mice were subjected to western blot-analysis with the indicated antibodies. Quantified data are presented in the *right graph*. Data are shown as mean ± SEM (n = 5) **P < 0.01 *versus* WT mice.

Figure 5. Response of *Ndrg2*-deficient astrocytes *in vitro*.

(A) Cell proliferation of WT or *Ndrg2*$^{-/-}$ astrocytes was analyzed by the MTT reduction assay at every 24 h up to day 5. Data are shown as mean ± SEM (n = 4). (B) The scratch wound assay was performed to evaluate cell migration by using cultured astrocytes isolated from WT or *Ndrg2*$^{-/-}$ mice. The quantification of cell migration was done by the measurement of coverage of the wound area at 24 h after scratching. Data are shown as mean ± SEM (n = 3). (C-E) Protein expression of Ndrg2 and GFAP in cultured astrocytes. Cells were stimulated with the indicated reagents for 48 h, and protein extracts were subjected to western blot analysis (C). The protein expression levels of Ndrg2 (D) and GFAP (E) under forskolin treatment were quantified. Data are shown as mean ± SEM (n = 4). *P < 0.05 *versus* control. Fsk: Forskolin, LPS: Lipopolysaccharide, ET1: Endothelin-1, TGFβ: Transforming growth factor-β. (F-H) Cultured astrocytes isolated from WT or *Ndrg2*$^{-/-}$ mice were stimulated by 10 μM forskolin. CRE reporter activity was determined by dual luciferase assay in astrocytes isolated from WT or *Ndrg2*$^{-/-}$ mice after the cultivation for 6 h in the presence or absence of 10 μM forskolin (F).

Gene expression levels were determined after 10 μM forskolin treatment for *Il6* (G) at 8 h and *Gfap* (H) at 24 h by qRT-PCR. **P < 0.05 *versus* astrocytes without forskolin treatment. $^{\#\#}$P < 0.01 *versus* indicated conditions. (I–L) Astrocytes isolated from WT or *Ndrg2*$^{-/-}$ mice were infected with the Ndrg2 adenovirus or LacZ adenovirus and cultured for 8 h in the presence or absence of 10 μM forskolin. Ndrg2 expression in *Ndrg2*$^{-/-}$ astrocytes was determined after adenovirus infection by qRT-PCR (I) and western blot (J). *Il6* expression in the cells and IL-6 secretion levels in cultured media were determined by qRT-PCR (K) and ELISA (L), respectively. Data are shown as mean ± SEM (n = 5–8). The values of IL-6 mRNA and protein in WT astrocytes stimulated with forskolin after infection of LacZ adenovirus were designated as hundred. $^{\#}$P < 0.05, $^{\#\#}$P < 0.01 *versus* indicated conditions.

Figure 6. Attenuated neuronal damage in *Ndrg2*-deficient mice after cortical stab injury. (A) Brain sections prepared from WT and *Ndrg2*$^{-/-}$ mice at day 4 after cortical stab injury were subjected to staining with FluoroJade C (*green*) or immunostaining with the anti-ssDNA antibody (*red*). *Scale bars* = 50 μm. Quantified data are presented in the *right graphs*. Data are shown as mean ± SEM (n = 5). *P < 0.05 *versus* WT mice. (B) Temporal gene expression profile for neuronal injury marker. The total RNA extracted from the ipsilateral and contralateral cortices of WT and *Ndrg2*$^{-/-}$ mice at day 1 to day 7 after injury was subjected to qRT-PCR with primers specific for *Atf3*. Data are shown as mean ± SEM (n = 3–4). *P < 0.05 *versus* indicated conditions.

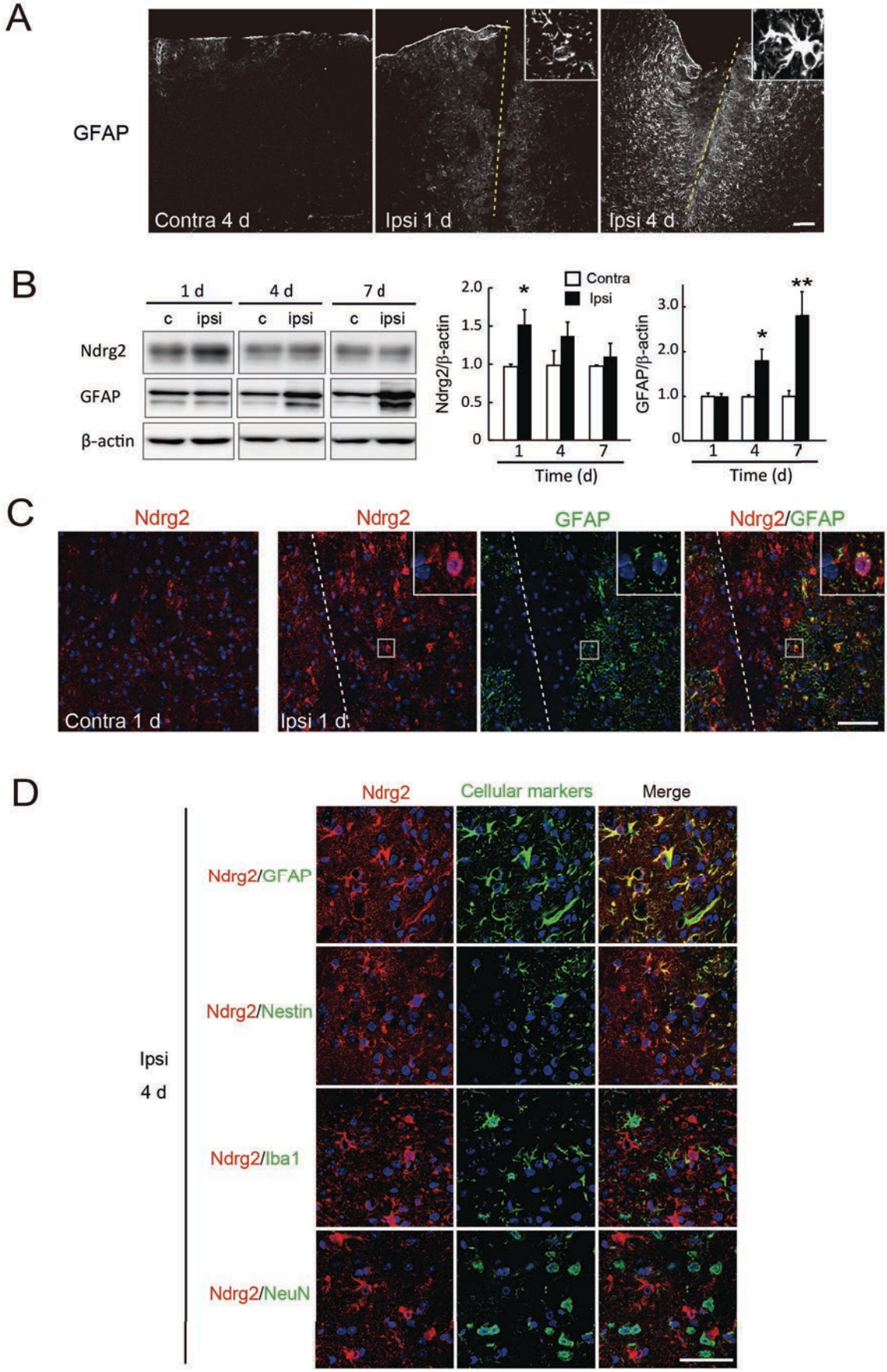

Fig. 1. *Takarada-Iemata et al.*

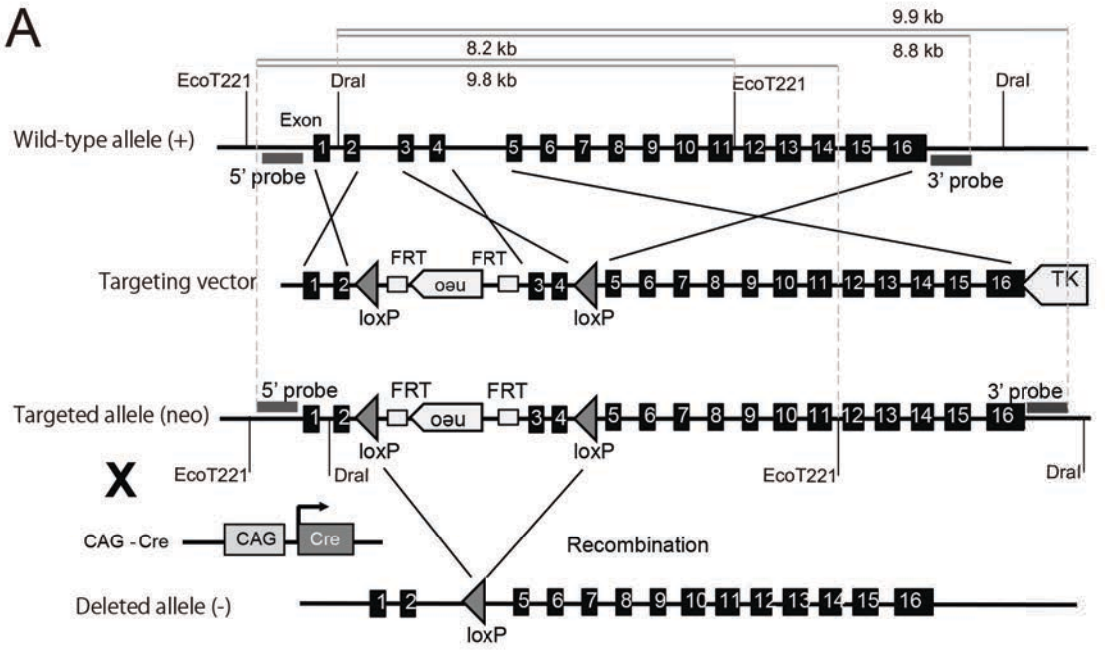

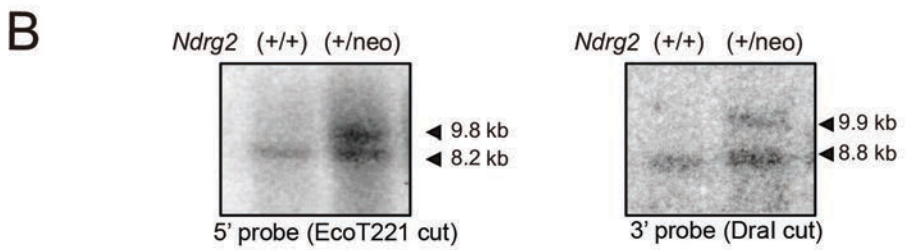

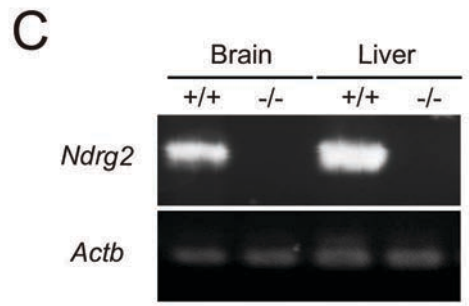

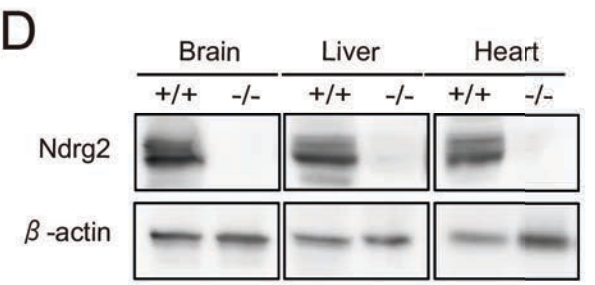

Fig. 2. *Takarada-Iemata et al.*

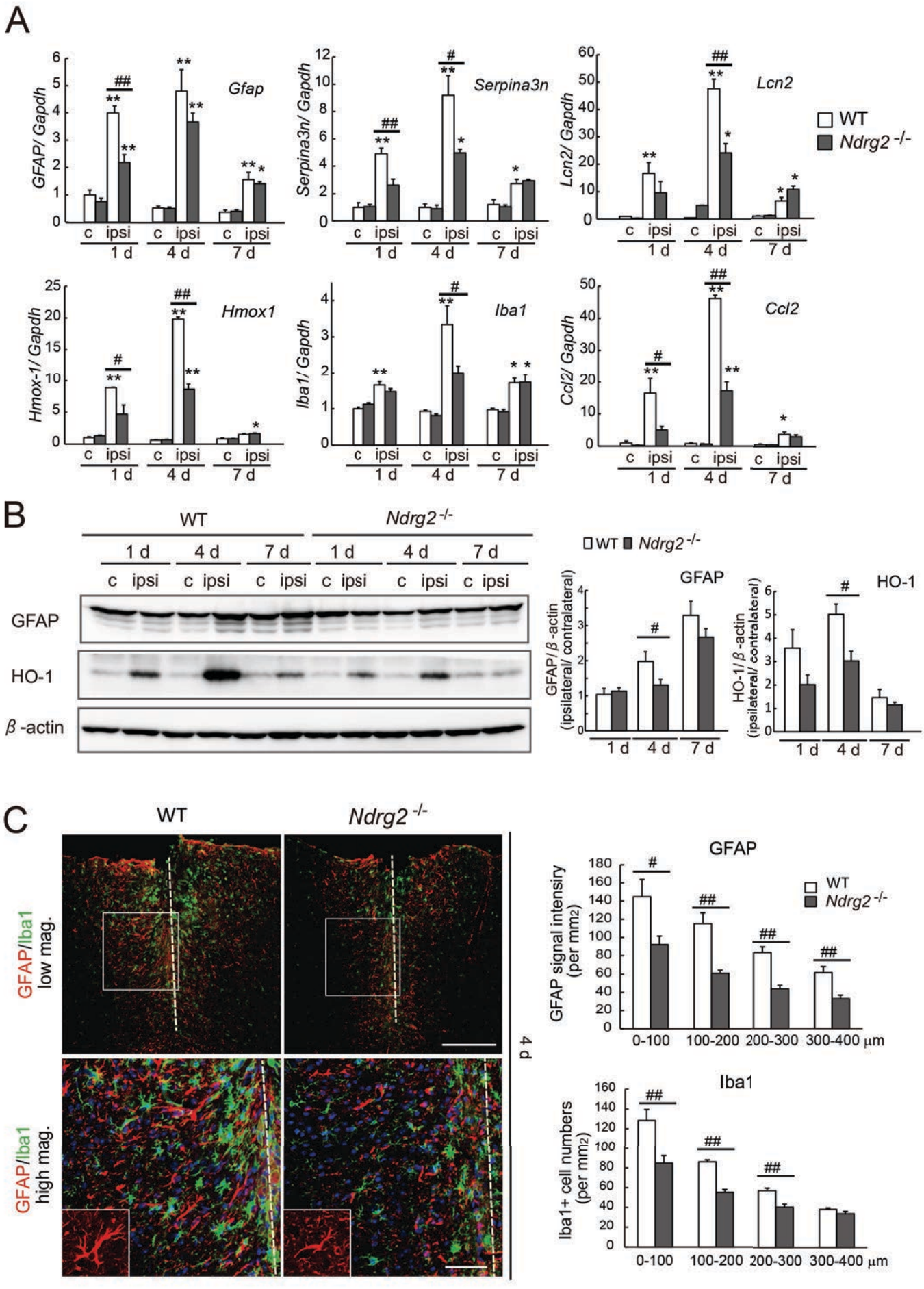

Fig. 3. *Takarada-Iemata et al.*

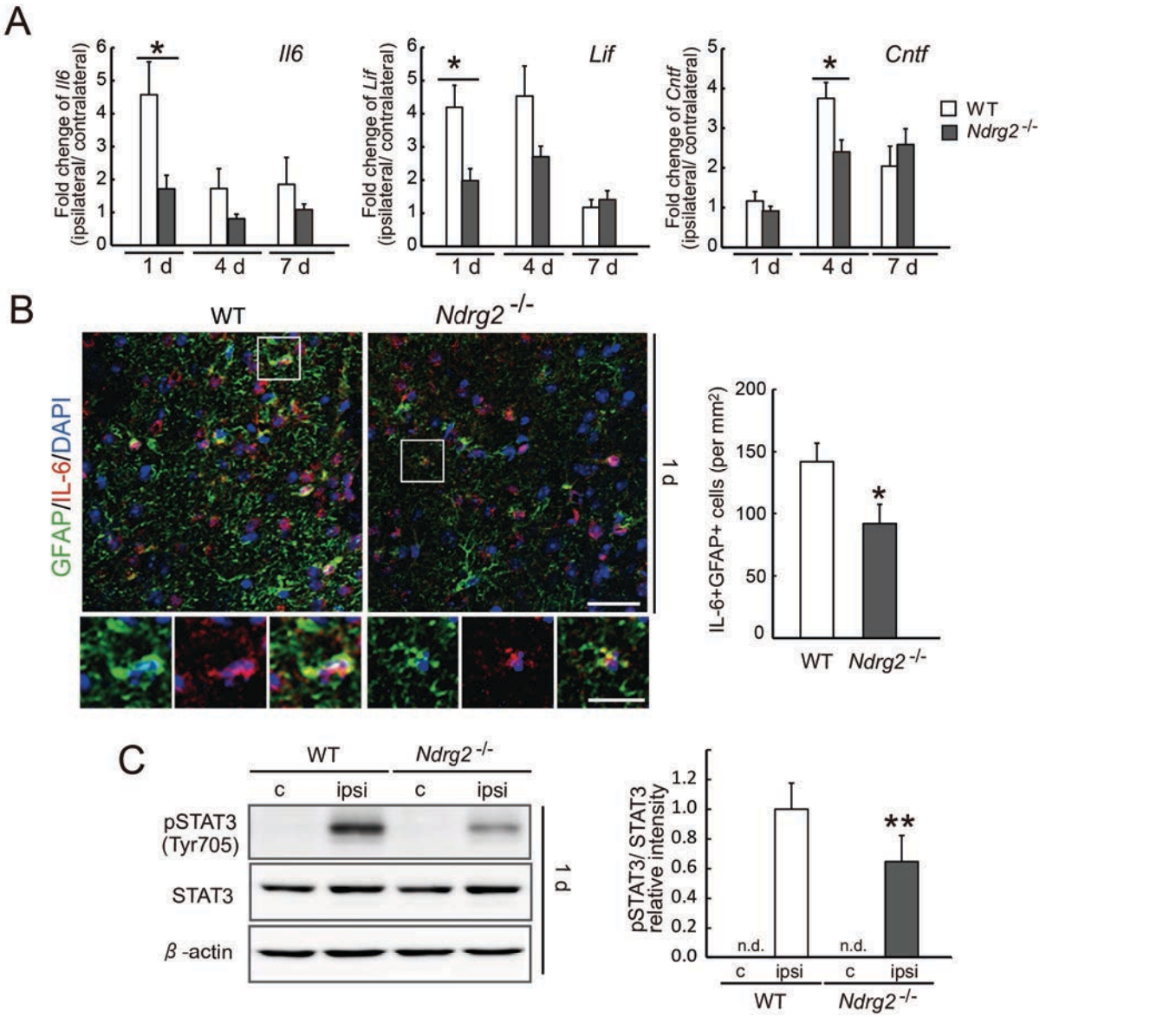

Fig. 4. *Takarada-Iemata et al.*

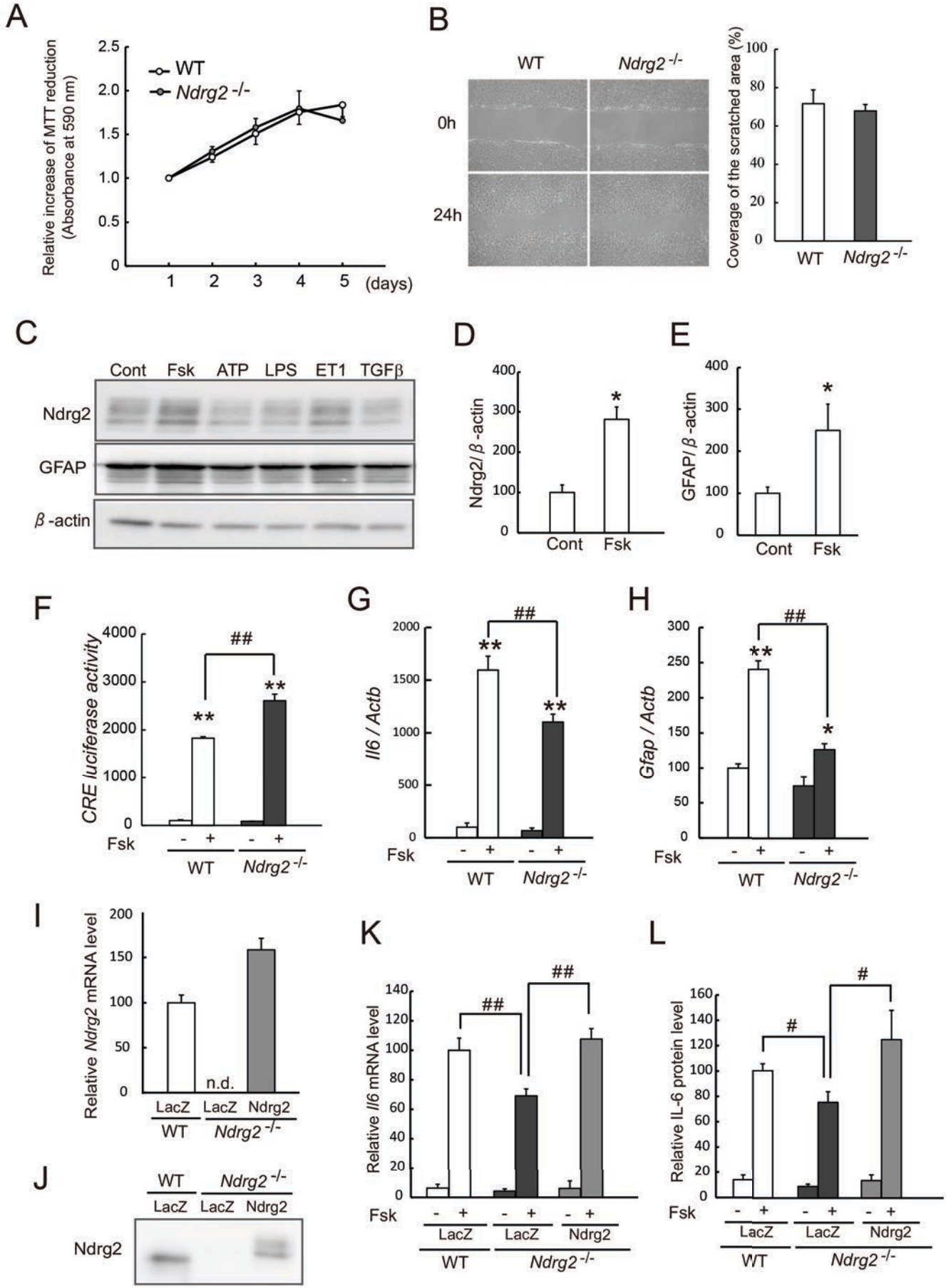

Fig. 5. *Takarada-Iemata et al.*

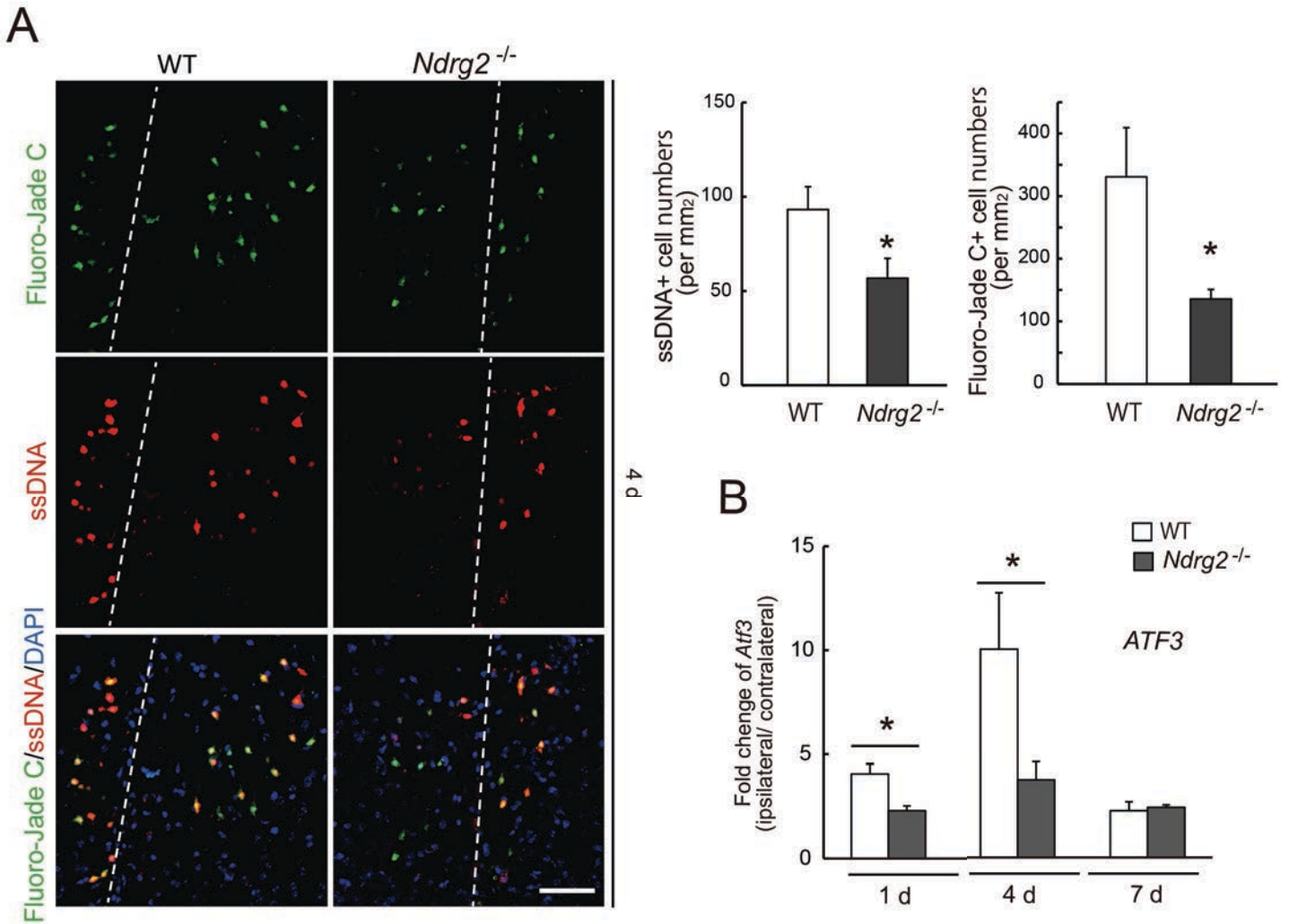

Fig. 6. *Takarada-Iemata et al.*

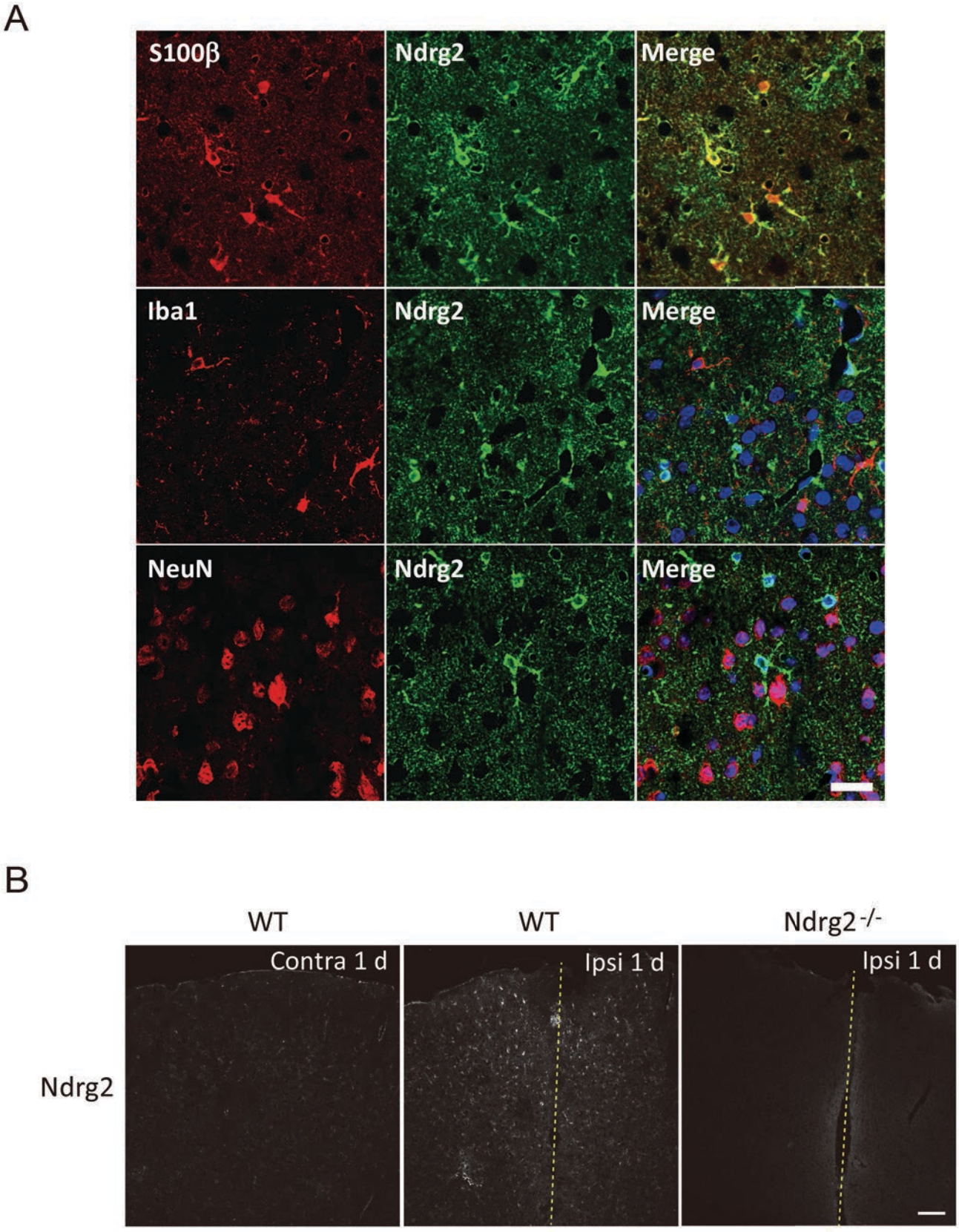

Supplemental Fig. 1 *Takarada-Iemata et al.*

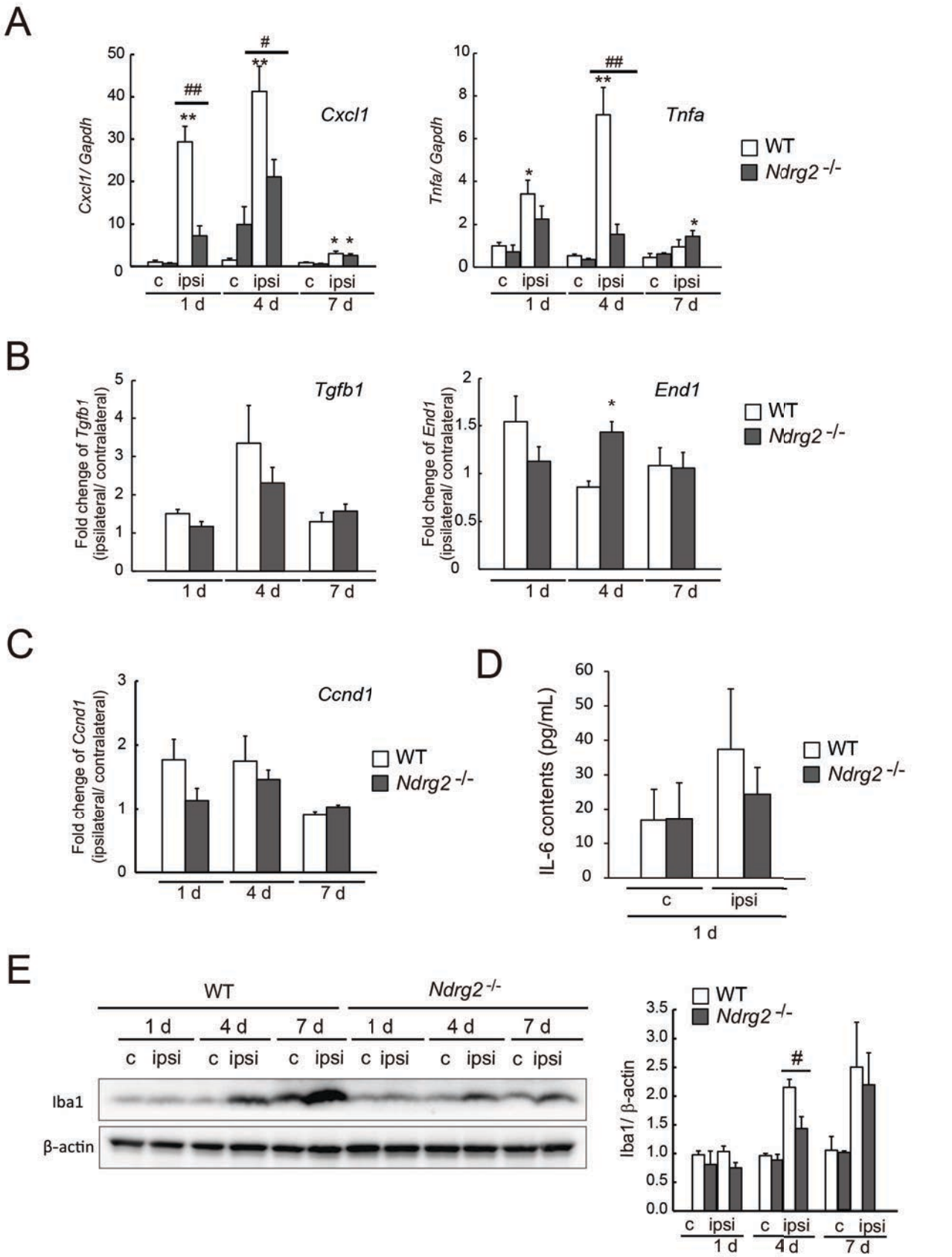

Supplemental Fig. 2 *Takarada-Iemata et al.*

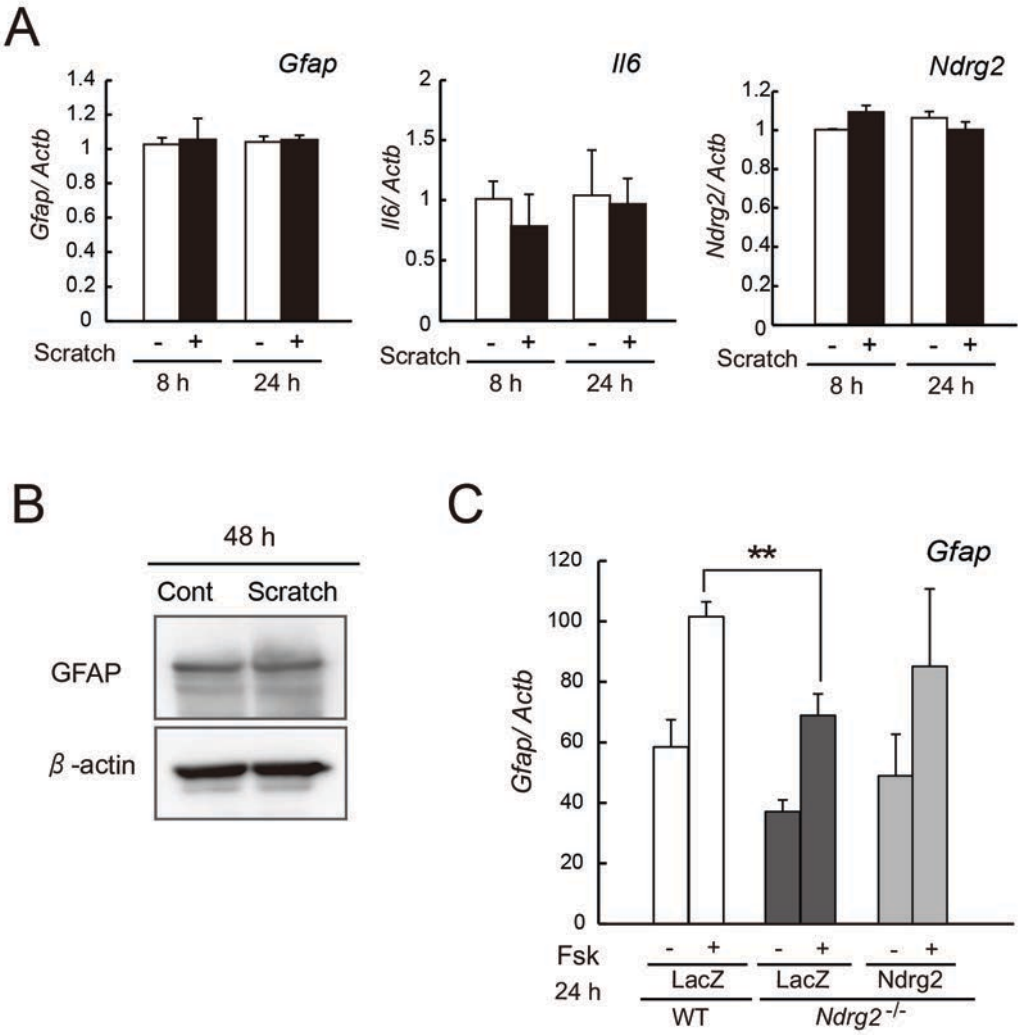

Supplemental Fig. 3 *Takarada-Iemata et al.*

Supplemental Table1. Primer sequences used for RT-PCR analysis

Genes	GenBank accession No.	Forward	Reverse	PCR Method
Ndrg2 ^{wt}		AGAGACTCTCTGACTTCCCT	CAAATGGAGAGACGGACACA	Traditional PCR
Ndrg2 ^{mut}		AGAGACTCTCTGACTTCCCT	TAGGTCCCTGCAAGAGGTTCACTA	Traditional PCR
Actb	NM_007393	GGTATCCTGACCCTGAAGTA	ATACAGGGACAGCACAGCCT	Traditional PCR
Ndrg2	NM_001145959	GCCTTACGTCTTCCATTCCGGA	CTTGAGGAACGAGGTCTGTG	Traditional PCR
Gapdh	NM_007393	AGGTCGGTGTGAACGGATTTG	TGTAGACCATGTAGTTGAGGTCA	Real-time PCR
Gfap	NM_001131020	CCCTGGCTCGTGTGGATTT	GACCGATACCACTCCTCTGTC	Real-time PCR
Lcn2	NM_008491	TGGAAGAACCAAGGAGCTGT	GGTGGGGACAGAGAAGATGA	Real-time PCR
Hmox1	NM_010442	AGGAGCTGCACCGAAGGGCTG	CGTGGAGACGCTTTACATAG	Real-time PCR
Iba1	NM_019467	CAGCAATGATGAGGATCTGC	CCAAGTTTCTCCAGCATTCG	Real-time PCR
Ccl2	NM_011333	CCAGCAAGATGATCCCAATG	TCTGGACCCATTCCTTCTTG	Real-time PCR
Il6	NM_031168	CCGGAGAGGAGACTTCACAG	TCCACGATTTCCCAGAGAAC	Real-time PCR
Lif	NM_001039537	CAACCTCATGAACCAGATCA	GATGGGAAGTCTGTCATGTT	Real-time PCR
Cntf	NM_170786	CTGGCTAGCAAGGAAGATTC	TCTGCCTCAGTCATCTCACT	Real-time PCR
Actb	NM_007393	TGTGATGGTGGGAATGGGTCAGAA	TGTGGTGCCAGATCTTCTCCATGT	Real-time PCR
Ndrg2	NM_001145959	ACACCTTATGGCTCGGTCAC	TCTCTTGCATATCCCCGAAC	Real-time PCR
Atf3	NM_007498	GAGGATTTTGCTAACCTGACACC	TTGACGGTAACTGACTCCAGC	Real-time PCR
Cxcl1	NM_008176	ACCCAAACCGAAGTCATAGC	TGGGGACACCTTTTAGCATC	Real-time PCR
Tnfa	NM_013693	CAAGCCTGTAGCCCACGTCG	ATCGGCTGGCACCACTAGTT	Real-time PCR
Tgfb1	NM_011577	CAATTCCTGGCGTTACCTTG	AGTGAGCGCTGAATCGAAAG	Real-time PCR
Edn1	NM_010104	AGGCCATCAGCAATAGCATC	AGTCAATGTGCTCGGTTGTG	Real-time PCR
Ccnd1	NM_007631	TGACACCAATCTCCTCAACG	ATGGCACAATCTCCTTCTGC	Real-time PCR